JACS
JOURNAL OF THE AMERICAN CHEMICAL SOCIETY

Communication

pubs.acs.org/JACS

The Functional Model Complex $[Fe_2(BPMP)(OPr)(NO)_2](BPh_4)_2$ Provides Insight into the Mechanism of Flavodiiron NO Reductases

Sheng Zheng,[†] Timothy C. Berto,[†] Eric W. Dahl, Melissa B. Hoffman, Amy L. Speelman, and Nicolai Lehnert*

Department of Chemistry, The University of Michigan, Ann Arbor, Michigan 48109-1055, United States

Supporting Information

ABSTRACT: Flavodiiron nitric oxide reductases (FNORs), found in many pathogenic bacteria, are able to detoxify NO by reducing it to N_2O. In this way, FNORs equip these pathogens with immunity to NO, which is a central immune defense agent in humans. Hence, FNORs are thought to promote infection of the human body, leading to chronic diseases. Despite this importance of FNORs for bacterial pathogenesis, the mechanism of NO reduction by these enzymes is not well understood. Here we present the synthesis and spectroscopic characterization of the diiron dinitrosyl model complex $[Fe_2(BPMP)(OPr)(NO)_2](BPh_4)_2$. The crystal structure of this complex shows two end-on-coordinated $\{FeNO\}^7$ units that, based on spectroscopic and electrochemical results, are only weakly electronically coupled. Importantly, reduction of this complex by two electrons leads to the clean formation of N_2O in quantitative yield. This complex therefore represents the first example of a functional model system for FNORs. The results provide key mechanistic insight into the mechanism of FNORs and, in particular, represent strong support for the proposed "super-reduced" mechanism for these enzymes.

Nitric oxide (NO) is a signaling molecule in mammals that is involved in blood pressure control and nerve signal transduction.[1] In addition, NO is produced by macrophages as a key immune defense agent to kill invading pathogens.[2] For the latter purpose, inducible NO synthase produces up to micromolar concentrations of NO, which is toxic against microbes.[3] However, recent research has shown that some pathogens (e.g., *Helicobacter pylori*, *Neisseria meningitides*, *Trichomonas vaginalis*, *Salmonella enterica*) have evolved defenses against NO toxicity by expressing flavodiiron nitric oxide reductases (FNORs) that are able to efficiently remove NO by reducing it to nontoxic N_2O.[4,5] This defense mechanism allows these pathogens to proliferate in the human body, causing harmful infections. FNORs therefore constitute significant targets for drug development. Despite their significance for microbial pathogenesis, the mechanism of these enzymes is not well understood.

FNORs belong to the family of flavodiiron proteins (FDPs), which are usually utilized to protect organisms against O_2.[6] These enzymes contain an N-terminal non-heme diiron active site, which is in close proximity of the C-terminal flavin mononucleotide (FMN) binding domain of an adjacent subunit. The non-heme diiron centers of FNORs show His/carboxylate

Scheme 1. Structural Comparison of the *Desulfovibrio gigas* FNOR Active Site (Top) and Model Complexes $[Fe_2(BPMP)(OPr)](BPh_4)_2$ (1, Bottom Left) and $[Fe(BMPA\text{-}PhO^{R,X})](OTf)$ (Bottom Right)

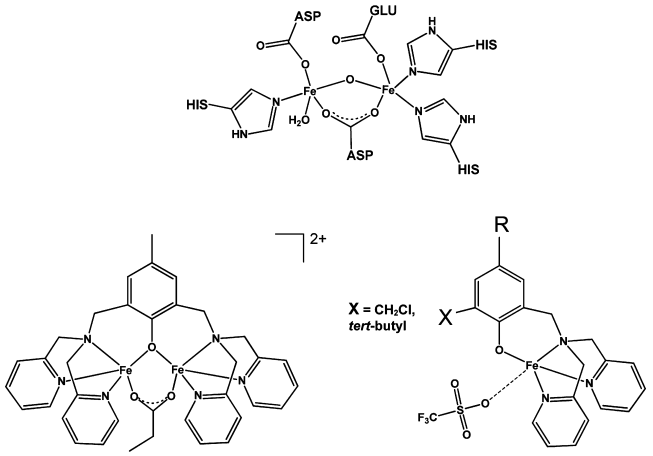

and water ligation (Scheme 1, top), which is typical for non-heme iron enzymes. However, one key difference is the presence of the redox-active FMN cofactor in very close proximity (~4 Å) to the diiron active site. Currently, the role of this cofactor for catalysis is unknown. Importantly, previous studies have shown that the ferrous non-heme iron centers in FNORs bind NO to generate typical high-spin $\{FeNO\}^7$ adducts with $S = 3/2$ total spin during turnover.[6,7] Several conflicting mechanisms have been proposed for FNORs, starting from either the mono- or dinitrosyl adducts of the diferrous form of the active site,[6,8] but evidence is now building up that the diferrous dinitrosyl, $[\{FeNO\}^7]_2$, is in fact the key intermediate for catalysis. Here we present the synthesis and spectroscopic characterization of the FNOR model complex $[Fe_2(BPMP)(OPr)(NO)_2](BPh_4)_2$, including its crystal structure. Excitingly, two-electron reduction of this complex leads to nearly quantitative formation of N_2O, making this complex the first functional model for FNORs. Finally, mechanistic implications for FNORs are discussed.

The diferrous complex $[Fe_2(BPMP)(OPr)](BPh_4)_2$ (**1**; see Scheme 1) was synthesized via previously reported methods with slight modification.[9] Addition of NO gas to an anaerobic solution of **1** causes an immediate color change to brown, indicating that $[Fe_2(BPMP)(OPr)(NO)_2](BPh_4)_2$ (**2**) has formed. Complex **2**

Received: October 3, 2012

 © XXXX American Chemical Society dx.doi.org/10.1021/ja309782m | *J. Am. Chem. Soc.* XXXX, XXX, XXX−XXX

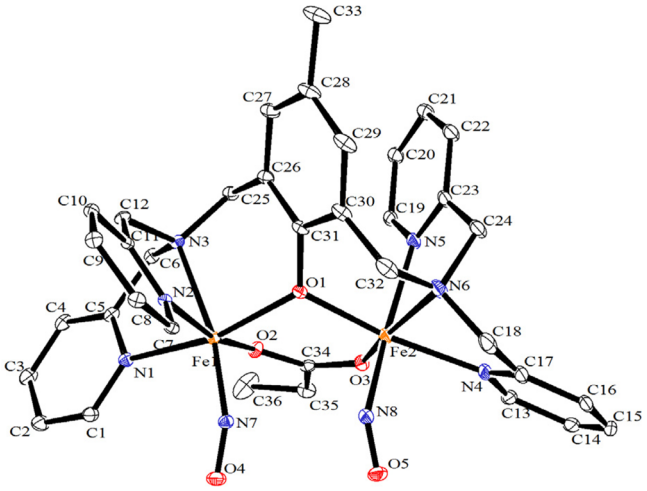

Figure 1. Crystal structure of **2** showing two NO molecules bound at the diiron core. The two BPh_4^- counterions have been omitted, along with all H-atoms, for clarity.

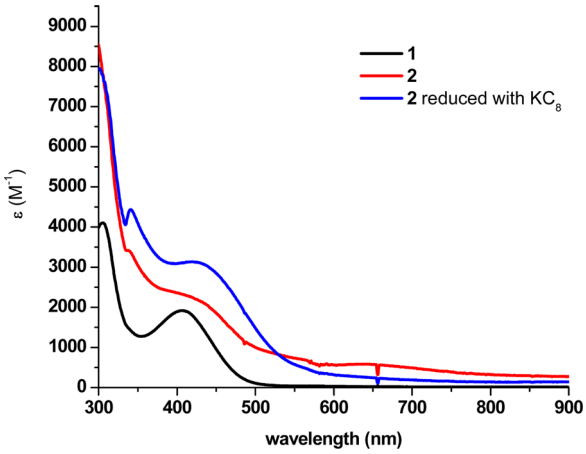

Figure 2. UV-visible absorbance spectra of **1**, **2**, and the corresponding reduction product generated concomitant with N_2O production. Recorded at room temperature in CH_2Cl_2.

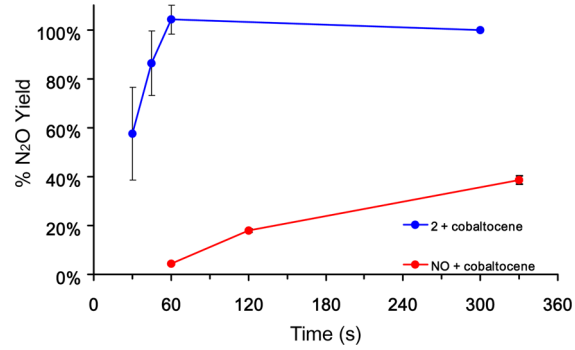

Figure 3. Percent N_2O formation at various reaction times for **2** in CH_2Cl_2 (blue) and dissolved NO (red) in the presence of cobaltocene.

exhibits long-term stability in solution under an NO atmosphere; however, in the absence of an NO atmosphere, **2** slowly loses NO over several days in solution. ^{1}H NMR and FT-IR spectra measured in $CDCl_3$ and CH_2Cl_2, respectively, show negligible decomposition within 1 h in room-temperature solution (see Supporting Information (SI), Figures S1 and S2). Two analogous monoiron complexes, [Fe(BMPA-PhO^{R,X})(NO)](OTf), with R = Me, X = CH_2Cl and R = X = ^{t}Bu (see Scheme 1), were also synthesized (see SI) to compare the reactivity of analogous mono- and dinuclear nitrosyl complexes (see below).

Structural characterization of **2** reveals a diiron dinitrosyl motif in which each iron center is coordinated by two pyridine units, a single NO moiety, and shared phenolate and propionate bridges to generate a pseudo-octahedral geometry at each iron center (see Figure 1). The two FeNO units within each molecule are geometrically distinct, with Fe−N(O) distances of 1.774 and 1.796 Å and Fe−N−O angles of 155.5° and 144.7° for Fe1 and Fe2, respectively. This is due to a nonsymmetric coordination of the BPMP ligand, where one NO moiety is *trans* to a tertiary amine (shorter Fe_1−NO bond) while the other is *trans* to the N-atom of a pyridine moiety (longer Fe_2−NO bond). Fe−O distances to the bridging phenolate moiety are 2.02 and 2.06 Å, with the longer Fe−O distance correlating with the more linear FeNO unit. The Fe−O bonds to the propionate moiety are also nonequivalent, at 1.997 and 2.067 Å, where the longer distance again corresponds to the more linear FeNO unit. The only other structurally characterized non-heme diiron dinitrosyl complex is $[Fe_2(Et\text{-}HPTB)(O_2CPh)(NO)_2](BF_4)_2$ (**3**), reported by Lippard and co-workers.[10] In comparison to **2**, **3** displays equivalent Fe−N(O) bonds at 1.750 Å and significantly less bent Fe−N−O units with an average angle of 167°.

The UV-visible absorption spectrum of **2** shown in Figure 2 displays a broad charge-transfer transition at 410 nm, in accordance with typical absorption features associated with non-heme {FeNO}^{7} complexes.[8b] Both {FeNO}^{7} units (each S = 3/2) in **2** are antiferromagnetically coupled, which is typically observed for [{FeNO}^{7}]$_2$ dimers in both enzymes and the above-mentioned model complex **3**.[11] Correspondingly, EPR spectroscopy at 4 K in frozen CH_2Cl_2 solution reveals that **2** is EPR-silent. Given the relatively small Fe−Fe distance of ∼3.5 Å and the presence of bridging ligands, the observed *magnetic (electron spin) coupling* between the iron centers is not surprising. For **3**, a coupling constant J = −23 cm^{-1} has been reported, which indicates quite strong exchange coupling between the Fe centers.

Although **2** shows two slightly nonequivalent Fe−N−O units, this complex is characterized by only one prominent N−O stretching feature at 1760 cm^{-1}, which shifts to 1686 cm^{-1} with $^{15}N^{18}O$. Nuclear resonance vibrational spectroscopy measurements on $[^{57}Fe_2(BPMP)(OPr)(NO)_2](BPh_4)_2$ display one isotope-sensitive feature at 487 cm^{-1} which is assigned to the ^{57}Fe−NO stretch. These N−O and Fe−NO frequencies agree well with previously published results for S = 3/2 high-spin mononuclear non-heme {FeNO}^{7} complexes.[12] Importantly, the observation of single N−O and Fe−NO stretching vibrations for **2** indicates that the two {FeNO}^{7} units in this complex are *electronically not very strongly coupled*.

Importantly, complex **2** does not mediate NO reduction and N_2O formation in solution, in agreement with previous observations for **3** and the dinitrosyl adducts of methane monooxygenase and ribonucleotide reductase, which are also not proficient in NO reduction.[8b] Excitingly, however, two-electron reduction of **2** by either chemical or electrochemical means causes rapid production of N_2O, as observed by IR spectroscopic analysis of the reaction headspace (see Figure S9). Integration of the N_2O stretching feature against a calibration curve generated from known N_2O gas standards reveals nearly quantitative N_2O formation after only 1 min in the presence of cobaltocene as reductant (see Figure 3). These results are obtained for a variety of chemical reductants including KC_8, decamethyl chromocene, and cobaltocene. By monitoring the corresponding metallocene

dx.doi.org/10.1021/ja309782m | J. Am. Chem. Soc. XXXX, XXX, XXX−XXX

oxidation, UV-visible absorption measurements show the initial reduction of **2** to be rapid, occurring within mixing time (~20 s; see Figure S16). Hence, the reduction of **2** is not rate limiting for N_2O generation. As mentioned above, ^{1}H NMR and solution IR measurements show **2** to be stable with respect to NO loss over a matter of hours in solution (see SI). The rapid reactivity upon the addition of reductant thus confirms that **2** is the active species that mediates N_2O generation. Reaction of NO gas with cobaltocene under similar conditions (as a control) leads to much slower N_2O formation, as shown in Figure 3, and a maximum N_2O yield of only ~40% under our experimental conditions. This further indicates that the reduction of NO to N_2O is in fact mediated by complex **2**.

As a further control, the complex [Fe(BMPA-PhO)(NO)](OTf) was synthesized as a monomeric analogue to **2** (see Scheme 1, R = Me, X = CH_2Cl, and SI). This complex displays a broad ν(N−O) band at 1782 cm^{-1} (Figure S7). Importantly, this monomeric analogue of **2** does not generate N_2O upon reduction with a slight excess of cobaltocene (reaction conditions are analogous to the reduction of **2**). However, we found this complex difficult to obtain in pure form, and in order to ensure that monomeric {FeNO}^{7} complexes are not capable of efficient N_2O generation, we further synthesized the complex [Fe(BMPA-^{t}Bu$_2$PhO)(NO)](OTf) (see Scheme 1, R = X = ^{t}Bu). IR and, in particular, EPR data (see Figures S19−S21) confirm that this complex is a pure, monomeric {FeNO}^{7} species. Treatment of this complex with reductant does not lead to N_2O generation after 15 min of reaction time, whereas N_2O generation is complete and quantitative with **2** after 1 min (see Figure 3). This further demonstrates that the diiron structure of **2** is essential for efficient N_2O formation. In agreement with this, no N_2O generation upon reduction of mononuclear {FeNO}^{7} species has been reported in the literature.

Interestingly, N_2O production via reduction of **2** is not a proton-dependent process and occurs in the absence of any external acid source. This finding is quite surprising, as the formation of water, i.e., $2NO + 2e^- + 2H^+ \rightarrow N_2O + H_2O$, could be envisioned as a thermodynamic driving force. As such, extreme care was taken to synthesize compound **2** in the strict absence of H_2O and using minimal alcohol throughout the entire metalation, nitrosylation, and reduction process (see SI). All solvents were distilled from CaH_2, and all solid reagents were vacuum-dried prior to use. Protic solvents are also not seen in the crystal lattice by XRD. Additionally, reduction of **2** in the presence of 4 equiv of acetic acid does not cause a noticeable increase in the reaction rate. This indicates that a sufficiently large thermodynamic driving force is available from N_2O generation without the need for protonation of the remaining oxo unit to form H_2O. In the absence of a proton source, NO reduction mediated by the diiron complex **2** might therefore proceed via formation of a bridging μ-oxo unit, i.e., $2Fe^{II}$−NO + $2e^- \rightarrow N_2O$ + Fe^{II}−O−Fe^{II}. The product is believed to take the form of a ferrous oxo-bridged cluster. While rare, similar complexes have been reported in the literature.[13] The yellow-brownish color of the reaction product, along with its absorption spectrum that lacks the characteristic broad absorption band of the air-oxidized (mixed-valent) form of **1** around 650 nm, supports this conclusion (see Figures 2 and S14). IR spectroscopy further shows that the reaction product lacks the NO ligand (see Figure S13), and ^{1}H NMR spectra taken at room temperature show chemical shifts similar to those observed for **1**, indicating that the reaction product also contains magnetically weakly coupled high-spin ferrous centers (see Figure S12). In contrast to **1**, oxidation

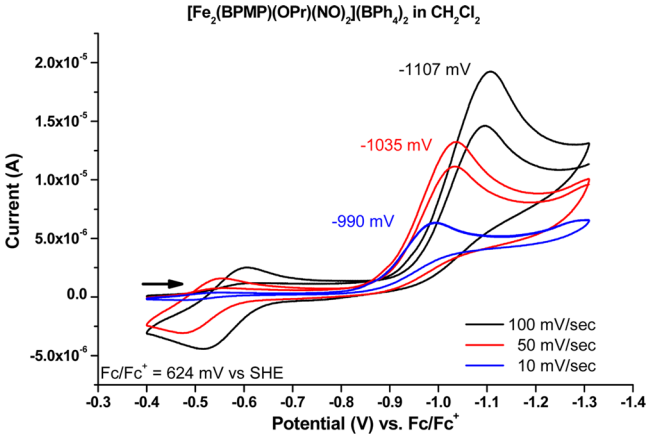

Figure 4. Sweep-rate-dependent cyclic voltammetry showing the irreversible reduction of **2** in CH_2Cl_2 vs Fc/Fc$^+$. Data taken at 50 and 100 mV/s show two consecutive scans, leading to the generation of the new signal at ~ −0.56 V.

of the reduction product by atmospheric O_2 is slow, indicating a coordinatively saturated structure. However, under weakly acidic conditions, which would be expected to disrupt an oxo bridge via protonation, air oxidation is quite rapid (see Figure S15). X-ray crystallography shows that the reaction product after acetic acid treatment corresponds to the diferrous complex with two acetate bridges, [Fe_2(BPMP)(Ac)$_2$](BPh$_4$)$_2$, which is isostructural to the analogous bis-propionate complex reported before.[9c]

Electrochemical potentials have been previously reported for [Fe_2(BPMP)(OPr)$_2$](BPh$_4$)$_2$, which is the bis-propionate-bridged analogue of **1**.[9a] Cyclic voltammetry measurements on **1** in CH_2Cl_2 under a N_2 atmosphere show two similar features associated with the $Fe^{II}Fe^{II}/Fe^{II}Fe^{III}$ and $Fe^{II}Fe^{III}/Fe^{III}Fe^{III}$ couples at 486 and 1198 mV vs Fc/Fc$^+$, respectively (see Figure S17). The large splitting between the two redox waves is indicative of a strong electronic interaction (coupling) between the iron centers. Curiously, however, the nitrosyl adduct **2** displays a single, irreversible reduction wave at −1.1 V vs Fc/Fc$^+$ (~ −0.5 V vs SHE). Upon reduction, a weak new feature appears at −0.56 V, which corresponds to the reaction product after denitrosylation of **2**, consistent with N_2O formation upon electrochemical reduction of **2** (Figure 4). Here, the scan-rate-dependent return of the −1.1 V reduction peak is due to diffusion of **2** to the electrode surface. Importantly, upon *bulk* two-electron reduction of **2** at −1050 mV (passing exactly 2 equivalents of charge), N_2O is detected in the gas headspace in high yield, further demonstrating that **2** is able to mediate NO reduction chemistry.

These results have direct mechanistic implications for FNORs and support the so-called "super-reduced" mechanism of NO reduction by these enzymes.[6,8b] This points to a specific role for the flavin cofactor, located in direct proximity to the diiron active site, for the catalytic mechanism of FNORs. We propose that direct two-electron reduction of the [{FeNO}^{7}]$_2$ intermediate of FNORs by the flavin cofactor is the central step of the catalytic mechanism that facilitates N_2O formation as shown in Scheme 2. In this respect, the observed weak electronic interaction between the two {FeNO}^{7} units in **2** is of key significance for this mechanism, as this avoids a large shift of the second reduction to very negative potentials, which would make it inaccessible to the flavin reductant. Hence, both reductions to generate the central [{FeNO}^{7}]$_2^{2-}$ intermediate (cf. Scheme 2) can be performed at similar, accessible potentials. Therefore, we propose that this step

dx.doi.org/10.1021/ja309782m | J. Am. Chem. Soc. XXXX, XXX, XXX−XXX

Scheme 2. Proposed Mechanism of NO Reduction by FNOR

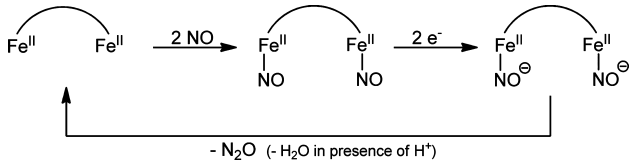

Scheme 3. Binding Mode of NO to Non-heme Diiron Centers and Its Effect on Reactivity

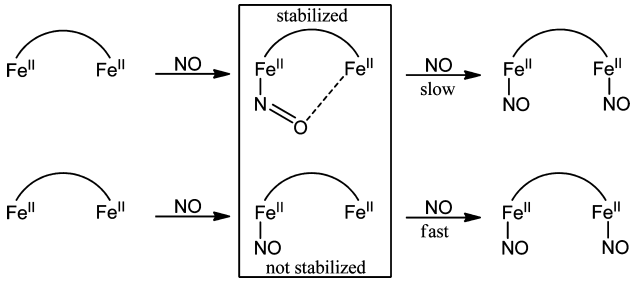

corresponds to a fast two-electron reduction on the basis of our findings for **2** (see Scheme 2).

In preliminary studies, we have also investigated the binding of NO to **1** by stepwise addition of NO, monitoring the reaction by EPR and IR spectroscopies. These data do not show preferential formation of a mononitrosyl complex but straightforward formation of the dinitrosyl **2**. This is in contrast to the preferential formation of a mononitrosyl adduct for deflavinated *Thermogata maritima* FDP. In this case, the mononitrosyl adduct is stabilized by a weak electrostatic interaction with the second iron center, as shown in Scheme 3, top.[8b,14] Curiously, a similar binding mode is observed for the mononitrosyl adduct of the O_2 carrier hemerythrin.[14] Consistent with this, the *T. maritima* FDP has been shown to be an O_2-reducing enzyme, as the NO reduction rate of this protein is low.[7] Based on these observations, we propose that the discriminating factor of whether an FDP functions as an efficient NO reductase or not lies in this difference in binding mode (see Scheme 3): whereas the O_2-reducing enzymes stabilize the mononitrosyl adduct and, in this way, prevent formation of the dinitrosyl, the NO-reducing enzymes do not show the semibridging binding mode of NO and, in this way, promote fast formation of the catalytically relevant dinitrosyl species, as shown in Scheme 3, bottom. In this respect, the ability of the O_2 reductases to bind diatomics in a bridging fashion can be envisioned to be advantageous for O_2 activation and reduction.

In conclusion, the diiron dinitrosyl adduct **2** has been prepared and spectroscopically characterized in this work. Reduction of **2** results in the liberation of N_2O in nearly quantitative yield, which directly supports the so-called "super-reduced" mechanism of NO reduction by FNOR enzymes. Future work will focus on testing the ability of **2** to mediate reduction of NO catalytically in an aqueous environment.[15]

■ ASSOCIATED CONTENT

Ⓢ Supporting Information

Synthetic procedures; UV-visible, IR, NMR, and NRVS spectra and CVs of **1** and **2**; N_2O headspace analysis; UV-visible, IR, and NMR spectra of the reaction product after N_2O formation; and tables of distances and angles and CIF file for **2**. This material is available free of charge via the Internet at http://pubs.acs.org.

■ AUTHOR INFORMATION

Corresponding Author

lehnertn@umich.edu

Author Contributions

†S.Z. and T.C.B. contributed equally to this work.

Notes

The authors declare no competing financial interest.

■ ACKNOWLEDGMENTS

This work was supported by the NSF (CHE 0846235). ALS acknowledges support from an NSF Graduate Research Fellowship (DGE-0718128). We acknowledge Dr. Jeff Kampf (University of Michigan) for X-ray crystallographic analysis of **2**.

■ REFERENCES

(1) (a) Lehnert, N.; Berto, T. C.; Galinato, M. G. I.; Goodrich, L. E. In *The Handbook of Porphyrin Science*; Kadish, K. M., Smith, K. M., Guilard, R., Eds.; World Scientific: Singapore, 2011; Vol. *14*, p 1. (b) *Nitric Oxide: Biology and Pathobiology*; Ignarro, L., Ed.; Academic Press: San Diego, 2000. (c) Wink, D. A.; Mitchell, J. B. *Free Radical Biol. Med.* **1998**, *25*, 434.

(2) Stuehr, D. J.; Gross, S. S.; Sakuma, I.; Levi, R.; Nathan, C. F. *J. Exp. Med.* **1989**, *169*, 1011.

(3) (a) Halpenny, G. M.; Heilmann, B.; Mascharak, P. K. *Chem. Biodiversity* **2012**, *9*, 1829. (b) Burney, S.; Tamir, S.; Gal, A.; Tannenbaum, S. R. *Nitric Oxide* **1997**, *1*, 130. (c) Long, R.; Light, B.; Talbot, J. A. *Antimicrob. Agents Chemother.* **1999**, *43*, 403. (d) Ouellet, H.; Lang, J.; Couture, M.; Ortiz de Montellano, P. R. *Biochemistry* **2009**, *48*, 863.

(4) (a) Baek, S.-H.; Rajashekara, G.; Splitter, G. A.; Shapleigh, J. P. *J. Bacteriol.* **2004**, *186*, 6025. (b) Missall, T. A.; Lodge, J. K.; McEwen, J. E. *Eucaryot. Cell* **2004**, *3*, 835. (c) Sarti, P.; Fiori, P. L.; Forte, E.; Rappelli, P.; Teixeira, M.; Mastronicola, D.; Sanciu, G.; Giuffré, A.; Brunori, M. *Cell. Mol. Life Sci.* **2004**, *61*, 618. (d) Stevanin, T. M.; Moir, J. W. B.; Read, R. C. *Infect. Immun.* **2005**, *73*, 3322.

(5) Gardner, A. M.; Helmick, R. A.; Gardner, P. R. *J. Biol. Chem.* **2002**, *277*, 8172.

(6) Kurtz, D. M., Jr. *J. Chem. Soc., Dalton Trans.* **2007**, 4115.

(7) (a) Silaghi-Dumitrescu, R.; Kurtz, D. M., Jr.; Ljungdahl, L. G.; Lanzilotta, W. N. *Biochemistry* **2005**, *44*, 6492. (b) Hayashi, T.; Caranto, J. D.; Wampler, D. A.; Kurtz, D. M., Jr.; Moenne-Loccoz, P. *Biochemistry* **2010**, *49*, 7040.

(8) (a) Blomberg, L. M.; Blomberg, M. R. A.; Siegbahn, P. E. M. *J. Biol. Inorg. Chem.* **2007**, *12*, 79. (b) Berto, T. C.; Speelman, A. L.; Zheng, S.; Lehnert, N. *Coord. Chem. Rev.* **2013**, *257*, 244.

(9) (a) Borovik, A. S.; Papaefthymiou, V.; Taylor, L. F.; Anderson, O. P.; Que, L., Jr. *J. Am. Chem. Soc.* **1989**, *111*, 6183. (b) Suzuki, M.; Kanatomi, H.; Murase, I. *Chem. Lett. Chem. Soc. Jpn.* **1981**, 1745. (c) Borovik, A. S.; Hendrich, M. P.; Holman, T. R.; Munck, E.; Papaefthymiou, V.; Que, L., Jr. *J. Am. Chem. Soc.* **1990**, *112*, 6031.

(10) Feig, A. L.; Bautista, M. T.; Lippard, S. J. *Inorg. Chem.* **1996**, *35*, 6892.

(11) (a) Coufal, D. E.; Tavares, P.; Pereira, A. S.; Hyunh, B. H.; Lippard, S. J. *Biochemistry* **1999**, *38*, 4504. (b) Haskin, C. J.; Ravi, N.; Lynch, J. B.; Munch, E.; Que, L., Jr. *Biochemistry* **1995**, *34*, 11090. (c) Lu, S.; Libby, E.; Saleh, L.; Xing, G.; Bollinger, J. M., Jr.; Moënne-Loccoz, P. *J. Biol. Inorg. Chem.* **2004**, *9*, 818.

(12) Berto, T. C.; Hoffman, M. B.; Murata, Y.; Landenberger, K. B.; Alp, E. E.; Zhao, J.; Lehnert, N. *J. Am. Chem. Soc.* **2011**, *133*, 16714.

(13) Baran, P.; Boca, R.; Chakraborty, I.; Giapintzakis, J.; Herchel, R.; Huang, Q.; McGrady, J. E.; Raptis, R. G.; Sanakis, Y.; Simopoulos, A. *Inorg. Chem.* **2008**, *47*, 645.

(14) Hayashi, T.; Caranto, J. D.; Hirotoshi, M.; Kurtz, D. M., Jr.; Moenne-Loccoz, P. *J. Am. Chem. Soc.* **2012**, *134*, 6878.

(15) This requires careful optimization of the experimental conditions to avoid direct reduction of NO gas by the applied reductant.

dx.doi.org/10.1021/ja309782m | *J. Am. Chem. Soc.* XXXX, XXX, XXX−XXX